Improvement of Data Embedding Method to Printed Image with High Detection Rate

Masashi Shiiba*, Takuhiro Nishikawa*, Mitsuji Muneyasu*, and Soh Yoshida*
*Faculty of Engineering Science, Kansai University
3-3-35 Yamate-cho, Suita-shi, Osaka, 564-8680, Japan

***Abstract*—To associate a printed medium with information on the Internet, several data embedding and detecting methods using the camera of a mobile device have been proposed. In these methods, a higher detection rate for the embedding data is required for practical use. This paper proposes an improvement of the data embedding method for achieving the higher detection rate. A new data embedding positions and a new method of generating embedding data are introduced. From an experiment, it is shown that the proposed method is effective for improving the detection rate.**

I. Introduction

When relating printed matter to information such as URLs, two-dimensional codes are widely used [1], [2]. In particular, mobile devises such as a smartphone can interpret the QR codes which is one of the major two-dimensional codes. However, there are problems with the use of two-dimensional codes. One is that an area for printing the code is required, and the other is that owing to the strong impression of the black and white pixels, the appearance of the printed matter may be impaired in some cases.

Therefore, data embedding techniques for embedding information in natural images instead of two-dimensional codes have been proposed [3], [4], [5]. For example, if you take a picture of a building in a campus map with your smartphone, you can receive a detail of the building. A watermarking technique is one of the foundations for these methods. However, the amount of information that can be embedded is small in the method proposed in [3], and the methods in [4] and [5] do not always achieve a high detection rate of the data. If we try to use these methods instead of the QR code, we need reliable information acquisition. For that purpose, the detection rate of the data should be as high as possible.

In [5], there are several causes for a decrease in the detection rate. One is that embedding data are generated by the sum of some Walsh codes. In the calculation of a correlation between the Walsh code and the embedded data at detecting, the correlation value is decreased compared to the value obtained by calculating the correlation between codes themselves. The reduction of the correlation value is related to the reduction of the detection rate. Another is the embedding position of data. The significant part of the embedding data is different according to the data to be embedded and may be placed in high-frequency components in the embedding position. The embedded data in the high-frequency position are easily damaged during printing and capturing processes. As a result, the detection rate may drop significantly depending on the embedded data.

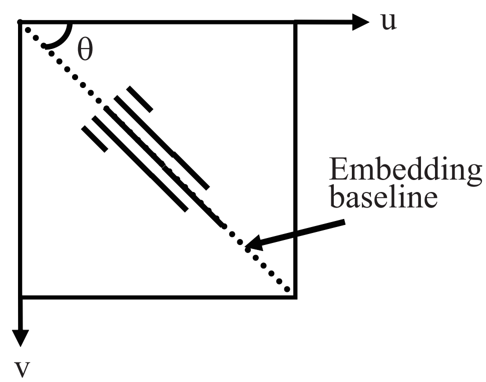

Fig. 1: Data embedding position of conventional method.

We propose a new method of achieving a higher detection rate. In this method, we introduce a new method for generating embedding data and a new position to embed the data. A gain adjustment method suitable for the proposed data embedding method is also developed. An experimental result shows that the proposed method can improve the detection rate effectively compared with the conventional method [5].

II. Conventional method [5]

The proposed method is based on the method proposed in [5]. We introduce the outline of the conventional method in the following.

A. Data embedding method

We divide an original image into 4×4 blocks, and a discrete cosine transform (DCT) is applied to each block. Next, we embed data in the intermediate-frequency region. Thereafter, a data-embedded image is obtained by applying an inverse discrete cosine transform (IDCT) to each block, concatenating the blocks, and adding a black frame border to the concatenated image.

1) Data embedding position: Data are embedded in the intermediate-frequency region on the embedding baseline drawn from the DC component at an angle of $\theta = 45°$ from the u-axis. Moreover, the same embedding sequence is embedded in three lines centered on this embedding baseline. The high-frequency parts of the left and right lines move to the adjacent low-frequency side. The embedding position is shown in Fig. 1.

2) Generation of embedding data: We describe the method of generating embedding data. Let the information to be embedded be $b_0, b_1, \cdots, b_{l-1}$, refferred to as an information bit sequence (IBS). The Walsh codes with 64 bits are used to generate the embedding data. The 63 Walsh codes (the 64 codes except the code with all 1's) are divided into 21 groups, each having three codes, and each group has a group number. Here, the group number corresponds to 4 bits of data, which we want to embed.

Therefore, the data representing an IBS can be generated as follows. First, an IBS is divided into 7 bits each. The first 4 bits of the 7 bits can be mapped to the group number. This 4-bit sequence is called a group bit sequence (GBS). Then the group number defines the codes in the group. The remaining 3 bits are embedded using these codes, and these bit sequences are referred as calls multi bit sequences (MBSs). If $b_i = 0$, the original code is used as it is, and if $b_i = 1$, the code is multiplied by -1.

The sum of these codes W is the data to be embedded into a block using $D_W = D + W \times g$, where D is the vector including the DCT coefficients at the positions to be embedded in the block, D_W is the vector including the embedded data, and g represents the gain which controls the strength of embedding. The gain also controls the image quality and data detectability.

3) Gain adjustment: The gain adjustment algorithm in the conventional method is as follows:

1) The initial value of the gain is set to 1.
2) The W corresponding to the IBS are embedded by $D_W = D + W \times g$.
3) The DCT coefficients at the embedding positions are extracted, and the correlation with each Walsh code is calculated.
4) The largest value of the difference between the correlation values for the codes used for embedding and the other codes is calculated.
5) If the value given by step 4 is greater than a predefined threshold, then go to step 6, otherwise, add 0.5 to the gain and go to step 2.
6) The adjustment of the gain progresses to the next block; go to step 1.

This algorithm is applied for each line in the embedding positions and each code in the group of the codes.

B. Data detecting method

In the detection processing, the frame border is first detected using the luminance component of the captured image. Next, to restore the geometric shape of the image, lens distortion correction, and projective transformation using the information obtained by detecting the frame border are performed. After the correction, the corrected image is divided into the same number of blocks like that in the embedding process. Each block is transformed into the frequency domain by the DCT.

For the transformed block, each code group should be distinguished. To distinguish between code groups, the absolute values of the correlation coefficients between data-embedded DCT coefficients and all the Walsh codes are used. Since the Walsh code is a type of orthogonal code, only the correlation of the data-embedded DCT coefficients with the embedding code is high. Therefore we calculate the correlation of the data-embedded DCT coefficients with the embedding codes in each group and the group whose value is largest is selected. The group number of the selected group is the GBS.

Then, the MBS is extracted by determining the correlation of the DCT coefficients with the Walsh codes in the determined group. That is,

$$\frac{\sum\sum(PR_i - \overline{PR}_i)(D_W - \overline{D}_W)}{\sqrt{\sum\sum(PR_i - \overline{PR}_i)^2 \sum\sum(D_W - \overline{D}_W)^2}} \tag{1}$$

is calculated, where PR_i, $\overline{PR}_i$ and $\overline{D}_W$ are the Walsh code, the average values of the Walsh code and the DCT coefficients in the embedded region, respectively. If this correlation is positive, the multi-bit is extracted as 0, and if negative, it is extracted as 1. Then, the MBS is determined. Finally, we take the majority from the obtained results to obtain the embedded data.

C. Problem of conventional method

The conventional method had a problem of a reduction of the data detection rate. The reasons for this problem are in the following.

1) Since embedding data are generated by the sum of some Walsh codes, the value of the correlation between the Walsh code and the embedded data at the detecting is decreased.
2) The significant part of the embedding data may be placed in high-frequency components in the embedding position. In this case, the embedded data in the high-frequency position are easily damaged during printing and capturing processes.

In this paper, we propose a new method for generating data to be embedded for the former problem and a new data embedding position for the latter.

III. Proposed Method

The proposed algorithm is similar to the conventional method in [5]. The details that are the same as in [5] are omitted.

A. Improvement of data embedding

1) Generation of embedding data: Here, we describe the method of generating embedding data. The Walsh codes with 64 bits are used to generate the embedding data, and the 63 Walsh codes (the 64 codes except the code with all 1's) are directly used for embedding the IBS. These codes correspond to the number from 0 to 126. The Walsh code w is the data to be embedded into a block using $D_w = D + w \times g$, In the case, since only one Walsh code is embedded, the number of the DCT coefficients to be modified is 64.

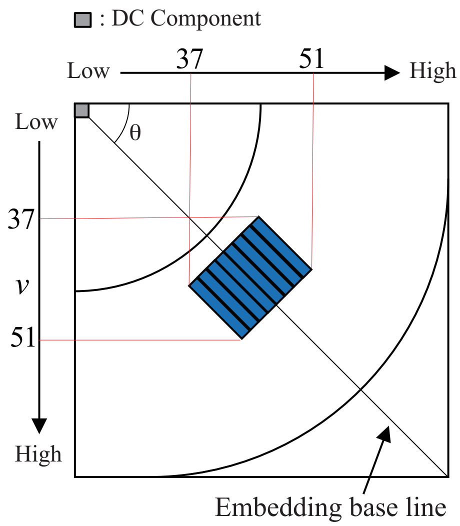

Fig. 2: Data embedding position.

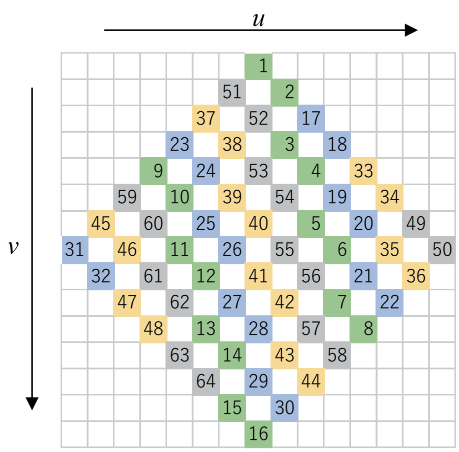

Fig. 3: Detail of data embedding position after scramble.

2) Data embedding position: The data embedding position is shown in Fig. 2. By embedding in the intermediate-frequency domain, we can avoid the deterioration of image quality. This position is determined by preliminary experiments.

Moreover, to avoid the deterioration of the data detection rate by burst damage, the embedding data are scrambled. Figure 3 shows in detail the positions of the embedding data after the scramble. The data are embedded at the coordinates $\{(u,v)|37 \leq (u,v) \leq 51\}$, where the block size is 128×128. Since the code length is 64, the data are embedded at positions 1 to 64 in Fig. 3.

3) Gain adjustment in data embedding: The gain is defined as follows. The correlations between D_w and all patterns of w are calculated. Let the largest correlation between w and D_w be C_w and the next largest correlation be C_L. Let th be a threshold. If $|C_w - C_L| < th$, then $g = g + 0.5$ and the data are embedded again. This procedure is repeated until $|C_w - C_L| > th$ is satisfied. The peak signal-to-noise ratio (PSNR) of each block is also calculated. The gain is also increased until the PSNR of each block exceeds a threshold.

This gain adjustment algorithm increases the gain to as high as possible while considering the quality of the embedded image. Therefore, the detection of embedded data can be robust. On the basis of preliminary experiments, we set th to 0.45 and the threshold of the PSNR to 41.5[dB].

B. Data detecting method

The detection processing is similar to the conventional method in [5]. The difference is that embedded data in each block are detected using w, which is a Walsh code. The DCT coefficients in the embedded domain are extracted from the DCT-transformed block, and the coefficients are sorted in their original order. Then, in the proposed method, we calculate the correlations between the sorted coefficients and all patterns of w, and the embedded IBS is determined from the w with the largest correlation value. Since we only embedded one Walsh code, the majority vote is not applied.

IV. Experiment

In this experiment, the data-embedded images created by the proposed method were printed and captured with a tablet. For printing and capturing, an LBP9600C (Canon) printer and a GALAXY Tab S SM-T700 tablet (Samsung) were used, and six images (Airplane, Lena, Mandrill, Milkdrop, Pepper, and Sailboat) of 512×512 pixels from the standard image database SIDBA were used. The size of each captured image was 1920×1080 pixels, the image was saved in Portable Network Graphics (PNG) format, and a total of 1380 images were created. As a performance measure, the detection rate $D_r(\%)$ is defined by $D_r = E_C/E_T \times 100$, where E_C is the number of bits of correctly detected data and E_T is the total number of bits of embedded data. $D_{100}(\%)$ is also defined by $D_{100} = D_p/D_a \times 100$, where D_p is the number of the captured image whose D_r is 100% and D_a is the total number of the captured images.

Table I shows the PSNR for each embedded image. In the following tables, (a), (b), (c), (d), (e), and (f) are Airplane, Lena, Mandrill, Milkdrop, Pepper, and Sailboat images, respectively. The PSNR of the images for the proposed method is almost the same as that for the conventional method [5]. Tables II, III show the average D_r in the case of each group-bit where the multi-bit fixed as "000". Tables IV, V show the average D_r in the case of each multi-bit where the group-bit fixed as "1110". In the proposed method, there is no discrimination of GBS and MBS; however, we introduce them in Tables III and V for the comparison with the conventional method. From these tables, the average D_rs of the proposed method are higher than that for the conventional method. Table VI shows that the comparison of the D_{100} of the conventional method and the proposed method. The value of the proposed method is higher than that of the conventional method. Thus, we confirm that the proposed method is effective and contributes to the improvement of the detection rate.

V. Conclusions

In this paper, we proposed an improvement in the data embedding method for achieving a higher detection rate. In particular, a method for generating embedding data and new

TABLE II: Average D_r of conventional method [5] for the case of each group-bit.

	0000	0001	0010	0011	0100	0101	0110	0111
(a)	100.00	100.00	100.00	100.00	100.00	100.00	99.11	100.00
(b)	100.00	100.00	100.00	100.00	100.00	100.00	99.55	100.00
(c)	100.00	100.00	100.00	100.00	100.00	100.00	98.39	100.00
(d)	100.00	100.00	100.00	100.00	99.82	100.00	99.82	99.82
(e)	99.02	98.13	100.00	99.02	99.91	99.46	99.20	97.50
(f)	96.88	92.59	99.11	93.93	95.36	90.00	95.45	88.57

	1000	1001	1010	1011	1100	1101	1110	1111	Ave.
(a)	99.64	99.91	96.16	99.91	94.82	99.37	96.16	97.86	98.93
(b)	97.50	99.46	97.59	97.50	98.12	99.91	93.48	98.30	98.84
(c)	98.84	100.00	97.59	100.00	99.46	99.82	97.86	97.68	99.35
(d)	97.05	100.00	96.52	100.00	98.66	98.84	95.00	97.50	98.94
(e)	99.55	100.00	98.30	99.91	97.14	98.66	99.20	98.75	98.98
(f)	95.45	93.30	95.18	91.16	94.55	98.93	87.23	95.89	93.976

TABLE III: Average D_r of proposed method for the case of each group-bit.

	0000	0001	0010	0011	0100	0101	0110	0111
(a)	100.00	100.00	100.00	100.00	100.00	100.00	100.00	100.00
(b)	100.00	99.20	100.00	100.00	100.00	100.00	100.00	100.00
(c)	100.00	100.00	99.46	100.00	100.00	100.00	100.00	100.00
(d)	100.00	100.00	100.00	100.00	100.00	100.00	100.00	100.00
(e)	100.00	100.00	100.00	100.00	100.00	100.00	100.00	100.00
(f)	100.00	100.00	100.00	100.00	100.00	100.00	100.00	100.00

	1000	1001	1010	1011	1100	1101	1110	1111	Ave.
(a)	100.00	100.00	100.00	98.66	100.00	100.00	100.00	100.00	99.92
(b)	100.00	100.00	100.00	100.00	100.00	100.00	100.00	100.00	99.95
(c)	100.00	100.00	100.00	100.00	99.64	100.00	98.39	100.00	99.84
(d)	100.00	100.00	100.00	100.00	100.00	100.00	100.00	100.00	100.00
(e)	99.91	100.00	100.00	100.00	100.00	100.00	100.00	100.00	99.99
(f)	100.00	99.73	100.00	100.00	100.00	99.64	100.00	100.00	99.96

TABLE I: PSNR of the conventional and proposed methods.

	[5]	Proposed
(a)	40.60	41.67
(b)	40.87	41.73
(c)	35.14	40.99
(d)	46.20	41.73
(e)	44.75	41.66
(f)	40.05	41.58

TABLE IV: Average D_r of conventional method [5] for the case of each multi-bit.

	001	010	011	100	101	110	111	Ave.
(a)	67.77	100.00	72.32	72.32	100.00	72.86	98.12	83.34
(b)	65.80	97.05	76.16	72.14	98.84	70.71	94.11	82.12
(c)	74.20	98.66	72.32	74.73	99.20	69.82	95.09	83.43
(d)	70.27	99.46	73.39	75.27	98.48	72.95	96.52	83.76
(e)	66.70	97.68	71.88	72.32	98.57	60.00	97.23	80.62
(f)	58.13	84.20	67.41	66.70	86.25	65.36	90.54	74.08

data embedding positions were introduced. Moreover, a gain adjustment algorithm suitable for the embedding method was developed. The improvement in detection rate was confirmed, experimentally.

TABLE V: Average D_r of proposed method for the case of each multi-bit.

	001	010	011	100	101	110	111	Ave.
(a)	100.00	100.00	100.00	100.00	100.00	100.00	100.00	100.00
(b)	100.00	100.00	100.00	100.00	100.00	99.82	100.00	99.97
(c)	99.29	100.00	100.00	99.55	100.00	95.98	100.00	99.26
(d)	100.00	100.00	100.00	100.00	100.00	100.00	100.00	100.00
(e)	100.00	100.00	100.00	98.21	100.00	100.00	100.00	99.74
(f)	100.00	99.11	99.64	100.00	100.00	100.00	100.00	99.82

TABLE VI: Comparison of D_{100} of the conventional and proposed methods.

	[5]	Proposed
D_{100}	47.39	97.11

ACKNOWLEDGEMENT

Part of this research was financially supported by a JSPS Grant-in-Aid for Scientific Research (C), (No.17K06450).

REFERENCES

[1] Z. Liu, "New Trends and Challenges in Digital Watermarking Technology: Applications for Printed Materials," in Multimedia Watermarking Techniques and Applications, B. Furht and D. Kirovski ed., pp.289–305, Auerbach Publications (2006).

[2] M. Muneyasu, "Data Embedding Techniques to Printing Images for Information Retrieving by Mobile Devices," Proc International Symposium on Multimedia and Communication Technology (2010), pp. 16–23.

[3] T. Nakamura, A. Katayama, M. Yamamuro, and N. Sonehara, "Fast Watermark Detection Scheme from Analog Image for Camera-Equipped Cellular Phone," Trans. IEICE (D-II), Vol.J87-D-II, no.12, pp.2145–2155 (2004) [in Japanese].

[4] M. Muneyasu, H. Kudo, T. Shono and Y. Hanada, "A Method of Data Embedding and Extracting for Information Retrieval Considering Mobile Devices," IEICE Trans. Fundamentals, Vol. E96-A, no.6, pp.1214–1221 (2013).

[5] A. Hiyama and M. Muneyasu, "Fast Information Retrieval Method from Printed Images Considering Mobile Devices," IEICE Trans. Fundamentals, vol. E96-A, no.11, pp.2194–2197, (2013).